Supporting Information

Petal-Like MoS_2 Nanosheets Space-Confined in Hollow Mesoporous Carbon Spheres for Enhanced Lithium Storage Performance

Xiue Zhang[a], *Rongfang Zhao*[a], *Qianhui Wu*[a], *Wenlong Li*[a], *Chao Shen*[a], *Lubin Ni*[a], *Hui Yan*[b], *Guowang Diao*[a]**, *Ming Chen*[a]*

[a]School of Chemistry and Chemical Engineering, Yangzhou University, Yangzhou, 225002, Jiangsu, China

[b]Department of Chemistry, University of Louisiana at Lafayette, Lafayette, LA 70504, United States of America

*E-mail address for corresponding authors: chenming@yzu.edu.cn, gwdiao@yzu.edu.cn

Supplementary Figures captions

Figure S1. FESEM and TEM images of (a, c) the SiO_2@SiO_2/RF nanospheres; and (b, d) the SiO_2@SiO_2/C nanospheres.

Figure S2. (a) BET nitrogen adsorption and desorption isotherms and (b) pore size distribution of the HMCSs with 20 nm thickness carbon shell; (c) BET nitrogen adsorption and desorption isotherms and (d) pore size distribution of the HMCSs with 65 nm thickness carbon shell.

Figure S3. FESEM images of the MoS_2@C nanospheres at different magnification.

Figure S4. TGA curves of the pure MoS_2 and MoS_2@C nanospheres.

Figure S5. BET nitrogen adsorption and desorption isotherms of the MoS_2@C nanospheres.

Figure S6. Schematic illustration of the formation of C@MoS_2 nanospheres.

Figure S7. (a) FESEM and (b, c) TEM images of the C@MoS_2 nanospheres.

Figure S8. (a) FESEM and (b, c) TEM images of the pure MoS_2 nanosheets.

Figure S9. (a) Survey XPS spectrum; (b-d) high resolution spectra of C1s, Mo3d, and S2p of the C@MoS_2 nanospheres.

Figure S10. TGA curves of the pure MoS_2 and C@MoS_2 nanospheres.

Figure S11. BET nitrogen adsorption and desorption isotherms of the C@MoS_2 nanospheres.

Figure S12. TEM images of (a-b) HMCSs with 65 nm thickness carbon shell, and (c) MoS_2/C nanospheres, TEM images of MoS_2/C nanospheres at reaction time of (d) 5 h, (e) 10 h, (f) 15h.

Figure S13. TEM images of WS_2@C.

Figure S14. TEM images of SnS_2@C.

Figure S15. Structure characterizations of the MoS_2@C after 200 GCD cycles at 1 A g^{-1}. (a, b) FESEM images at different magnification; (c-f) Annular dark-field STEM image, and the corresponding EDX elemental mappings of C, Mo, S.

Figure S16. TEM images of the MoS_2@C nanospheres (a, b) after 200 GCD cycles at 1 A g^{-1}.

Figure S17. Structure characterizations of the C@MoS_2 anode after 200 GCD cycles at 1 A g^{-1}. (a, b) FESEM and (c, d) TEM images at different magnification; (e-h) Annular dark-field STEM image, and the corresponding EDX elemental mappings of C, Mo, S.

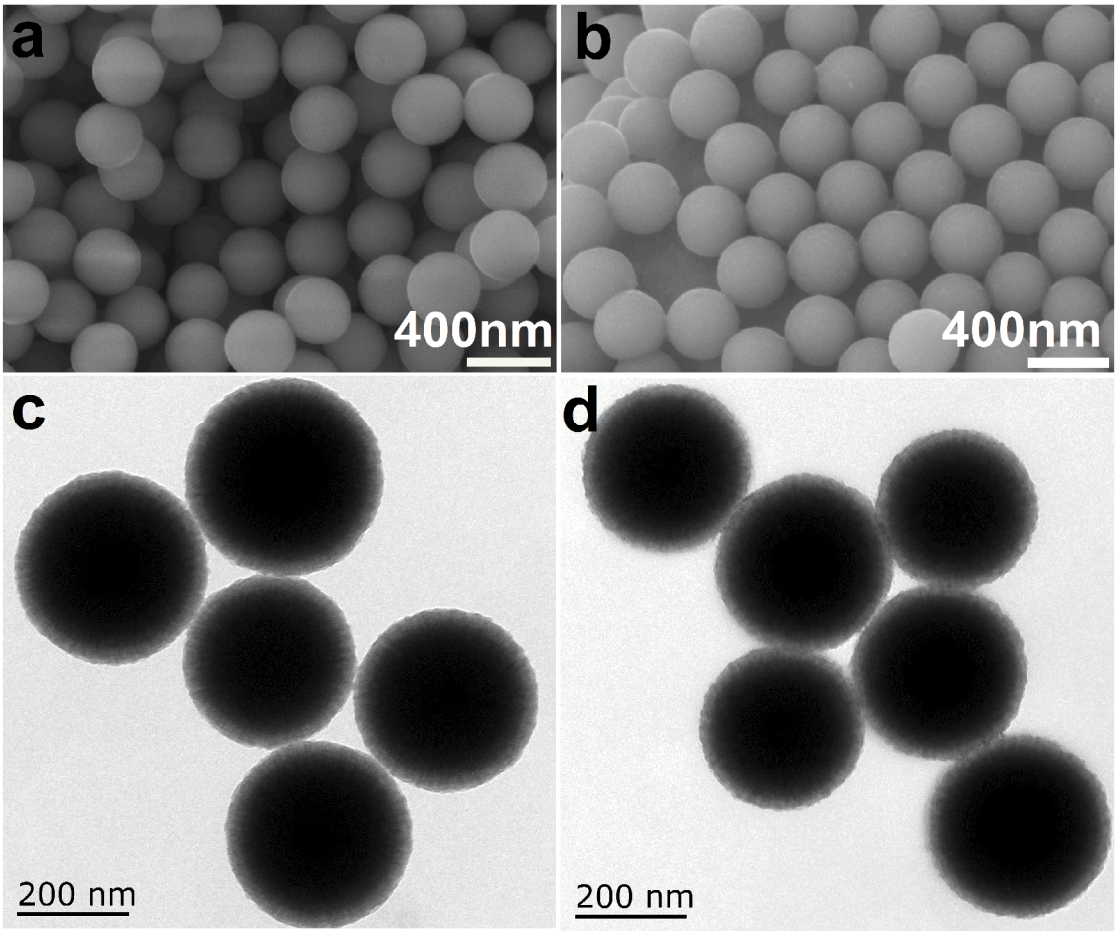

Figure S1. FESEM and TEM images of (a, c) the SiO_2@SiO_2/RF nanospheres; and (b, d) the SiO_2@SiO_2/C nanospheres.

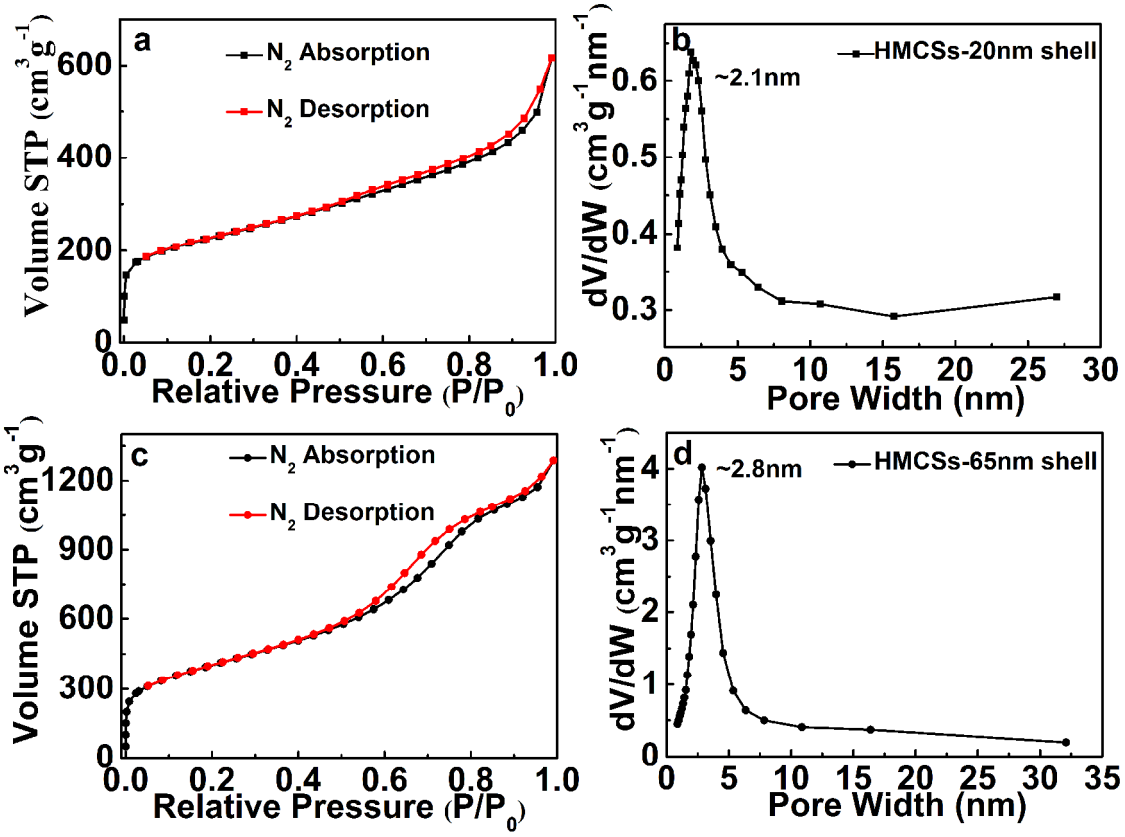

Figure S2. (a) BET nitrogen adsorption and desorption isotherms and (b) pore size distribution of the HMCSs with 20 nm thickness carbon shell; (c) BET nitrogen adsorption and desorption isotherms and (d) pore size distribution of the HMCSs with 65 nm thickness carbon shell.

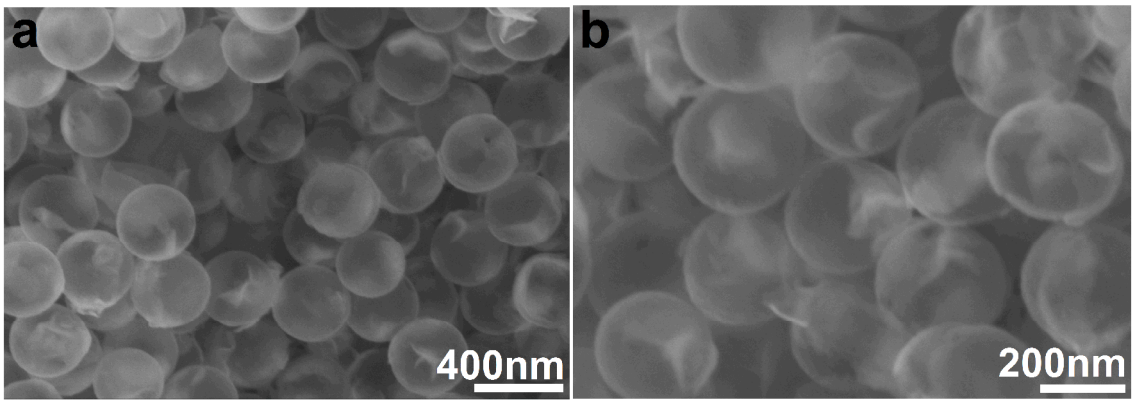

Figure S3. FESEM images of the MoS_2@C nanospheres at different magnification.

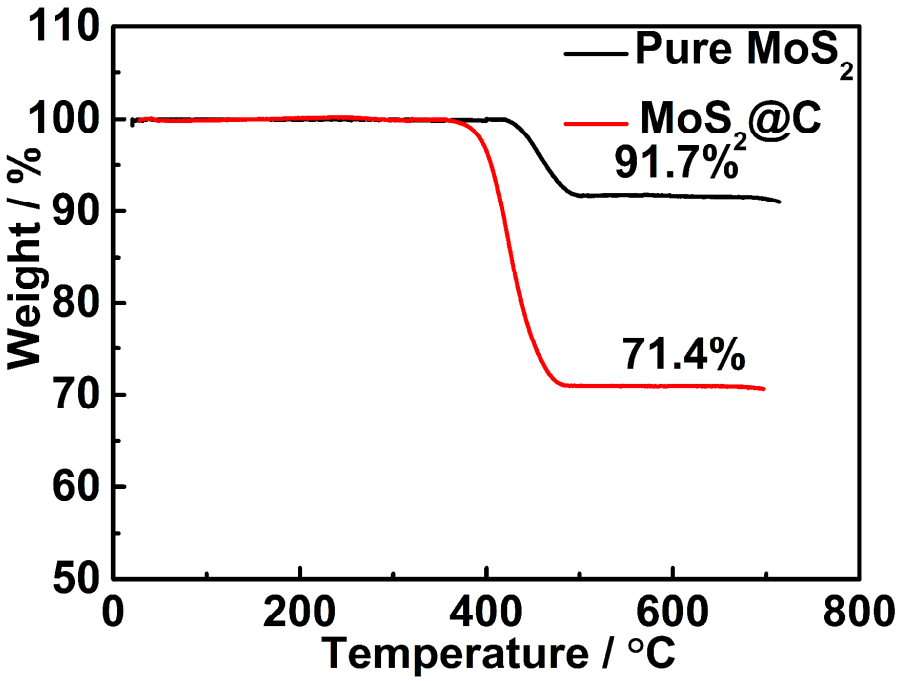

Figure S4. TGA curves of the pure MoS_2 and MoS_2@C nanospheres.

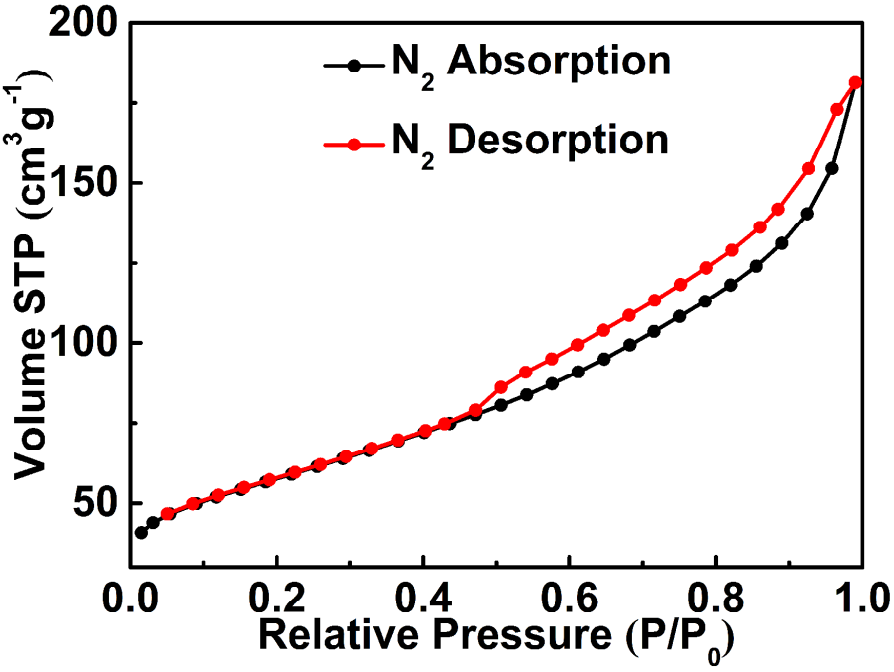

Figure S5. BET nitrogen adsorption and desorption isotherms of the MoS_2@C nanospheres.

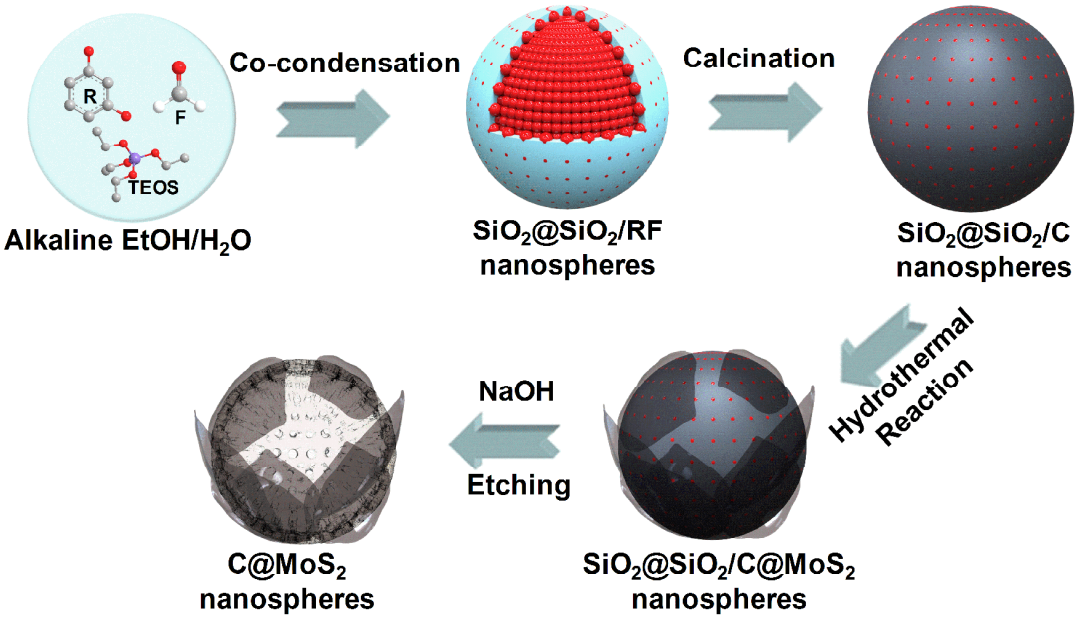

Figure S6. Schematic illustration of the formation of C@MoS_2 nanospheres.

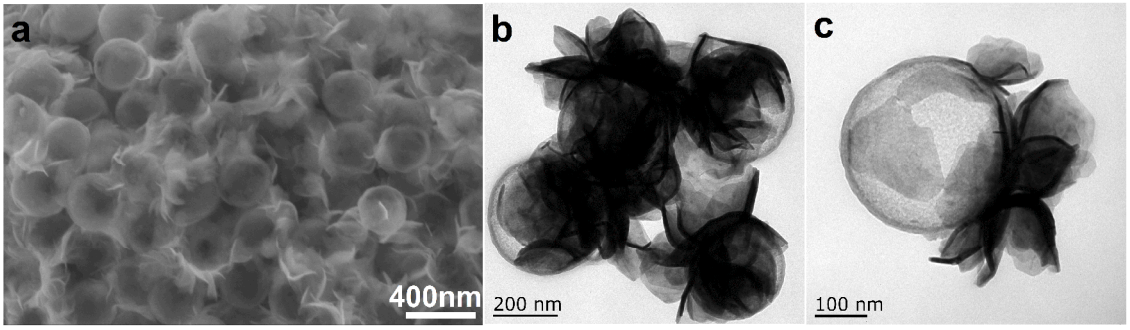

Figure S7. (a) FESEM and (b, c) TEM images of the C@MoS_2 nanospheres.

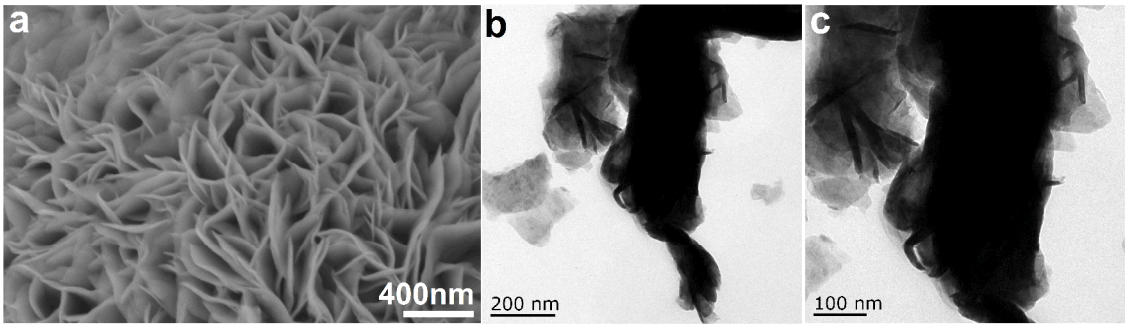

Figure S8. (a) FESEM and (b, c) TEM images of the pure MoS_2 nanosheets.

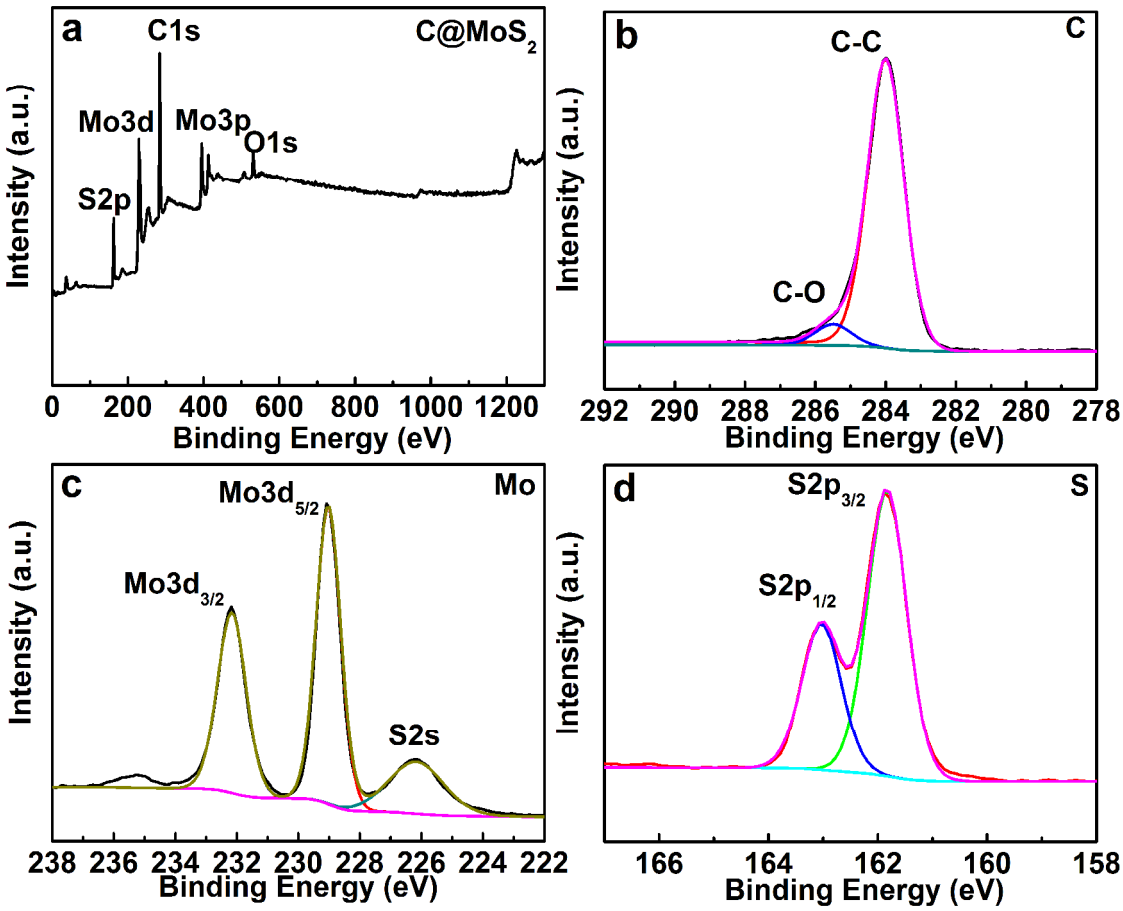

Figure S9. (a) Survey XPS spectrum; (b-d) high resolution spectra of C1s, Mo3d, and S2p of the C@MoS_2 nanospheres.

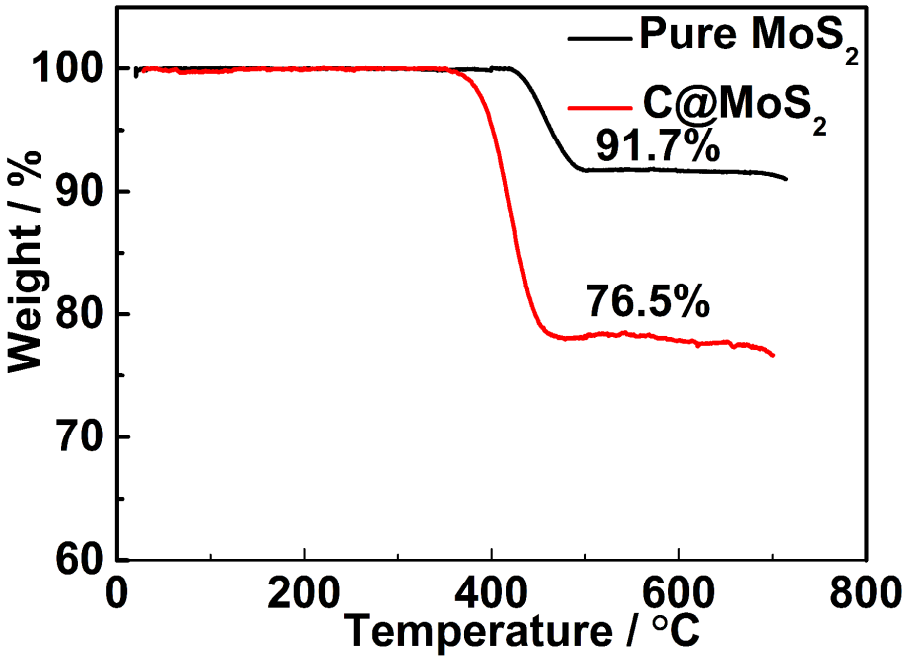

Figure S10. TGA curves of the pure MoS_2 and C@MoS_2 nanospheres.

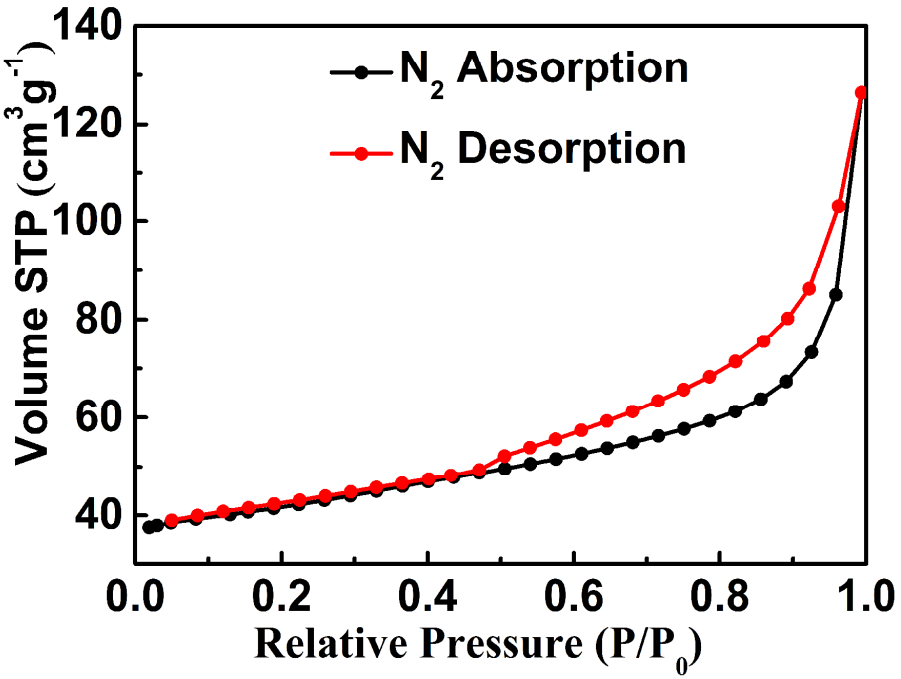

Figure S11. BET nitrogen adsorption and desorption isotherms of the C@MoS_2 nanospheres.

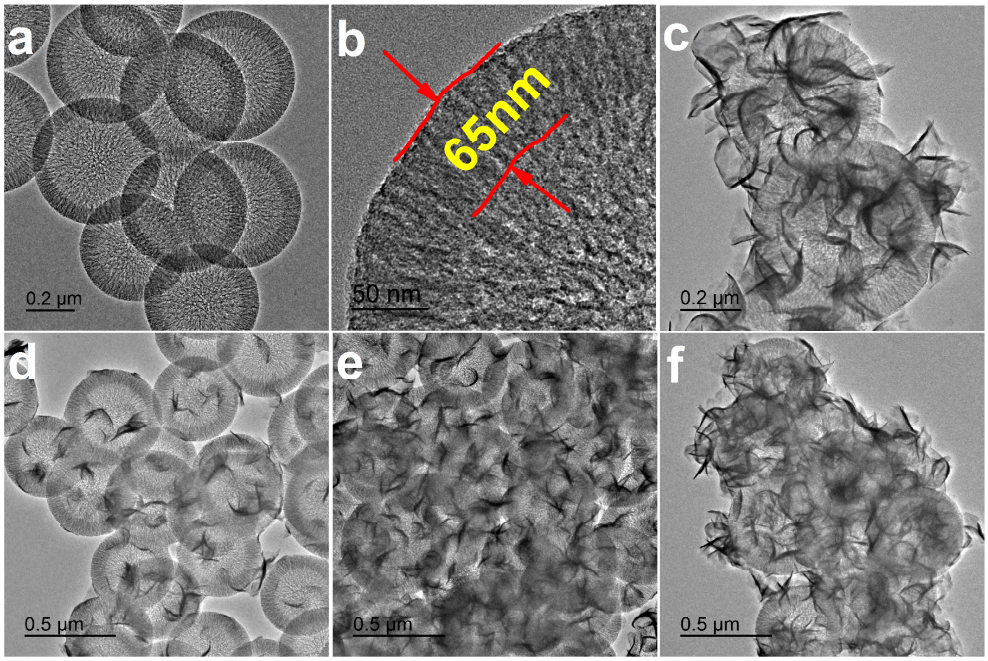

Figure S12. TEM images of (a-b) HMCSs with 65 nm thickness carbon shell, and (c) MoS_2/C nanospheres, TEM images of MoS_2/C nanospheres at reaction time of (d) 5 h, (e) 10 h, (f) 15 h.

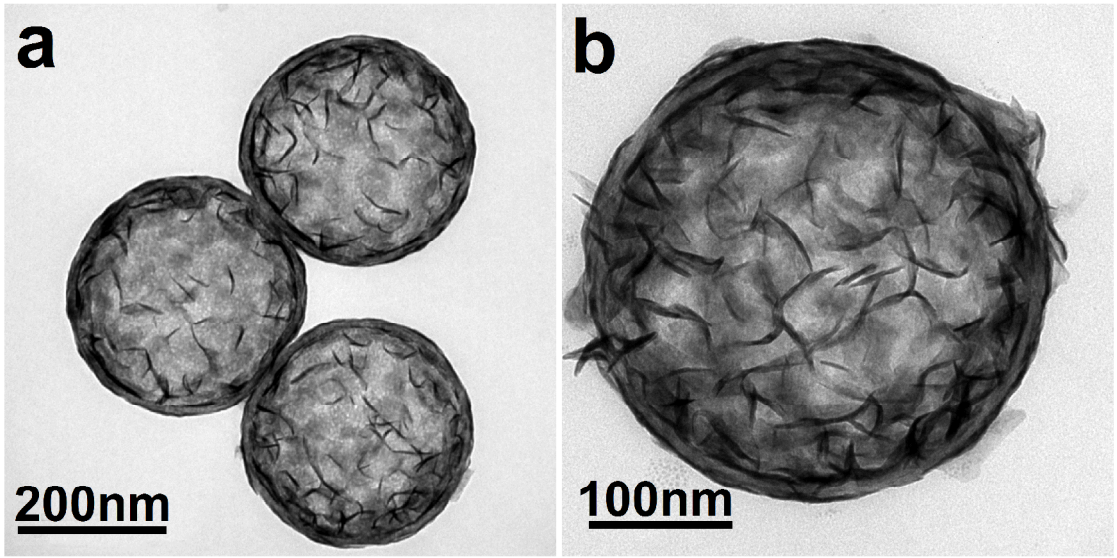

Figure S13. TEM images of WS_2@C.

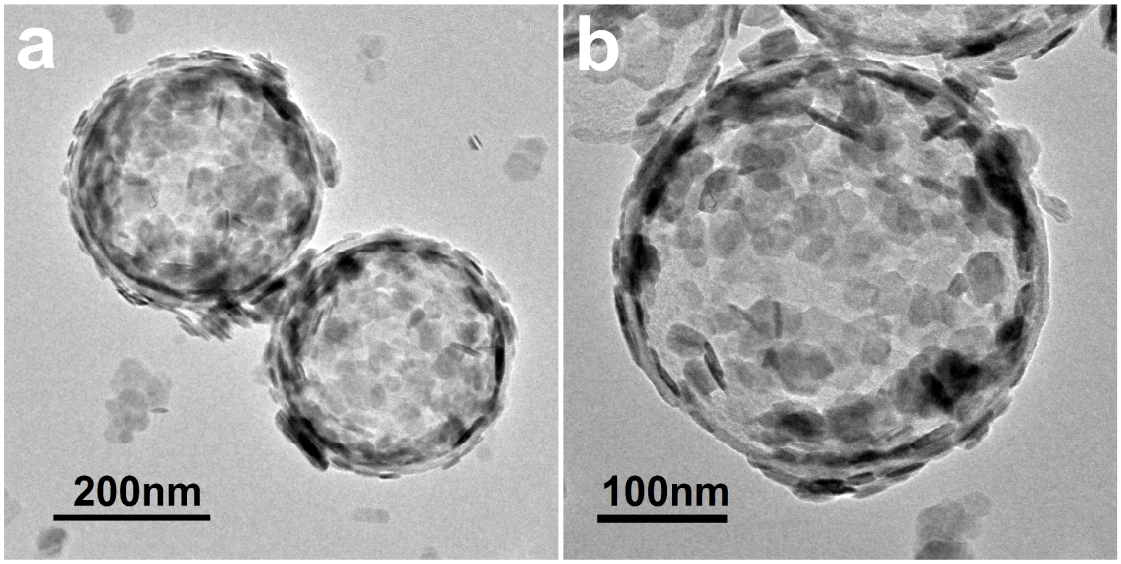

Figure S14. TEM images of SnS_2@C.

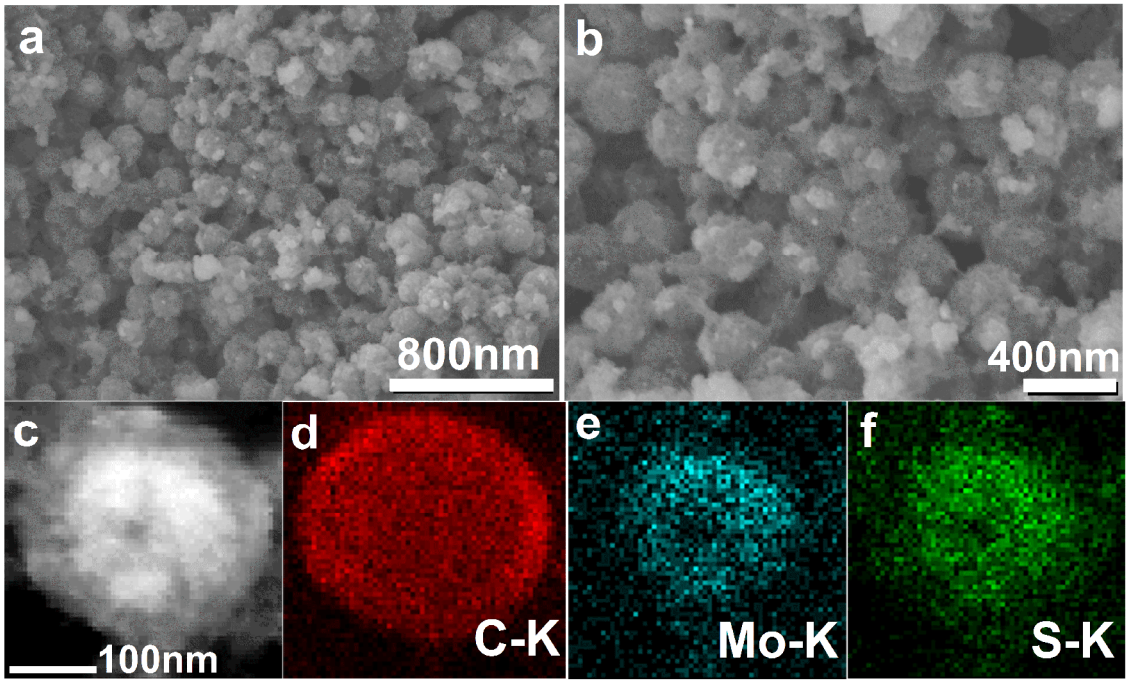

Figure S15. Structure characterizations of the MoS_2@C after 200 GCD cycles at 1 A g^{-1}. (a, b) FESEM images at different magnification; (c-f) Annular dark-field STEM image, and the corresponding EDX elemental mappings of C, Mo, S.

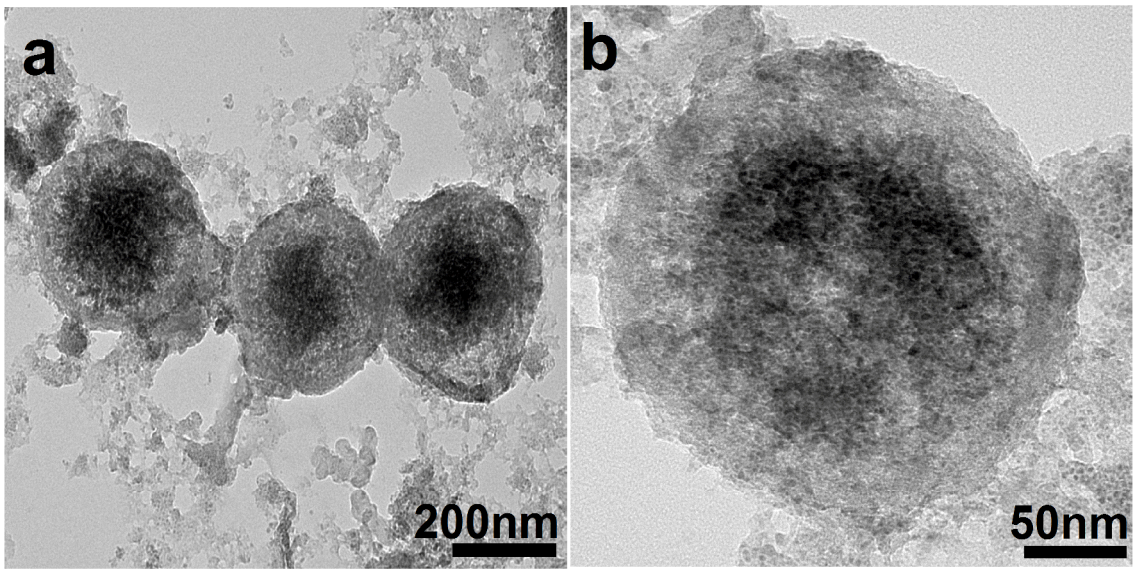

Figure S16. TEM images of the MoS_2@C nanospheres (a, b) after 200 GCD cycles at 1 A g^{-1}.

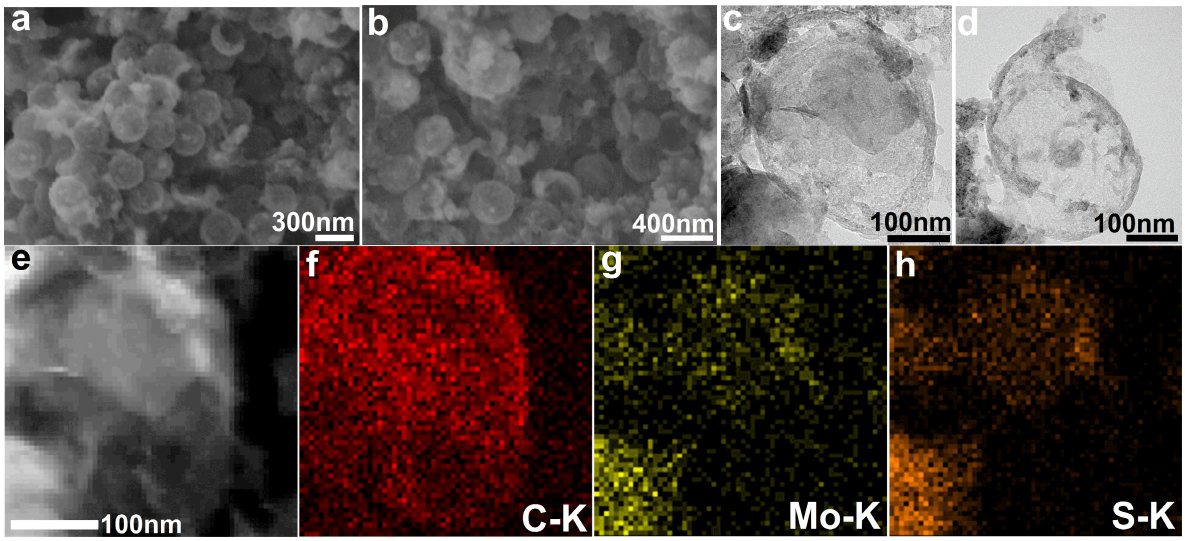

Figure S17. Structure characterizations of the C@MoS_2 anode after 200 GCD cycles at 1 A g^{-1}. (a, b) FESEM and (c, d) TEM images at different magnification; (e-h) Annular dark-field STEM image, and the corresponding EDX elemental mappings of C, Mo, S.

Table S1. Summary of electrochemical performances of different MoS_2-based anodes.

Sample	**Current density ($A\ g^{-1}$)**	**Initial discharge/charge capacity ($mA\ h\ g^{-1}$)**	**Reversible capacity ($mA\ h\ g^{-1}$)/ Cycles/Current density ($A\ g^{-1}$)**	**References**
Yolk/shell MoS_2@C	1	1671/1197	993/200/1 624/400/5	This work
Hierarchical MoS_2–C microspheres	0.2	1200/980	780/100/1	[1]
Hierarchical MoS_2@Carbon Microspheres	0.5	1050/809	650/300/1	[2]
C@MoS_2 nanoboxes	1	1966/1164	952/200/0.4 1233/50/0.1	[3]
Hollow carbon with a few-layered MoS_2-entrapped	0.05	1134/835	969/100/0.5 822/200/1	[4]
Quasi-hollow C@MoS_2	0.1	857/566	652/100/0.1	[5]
Nitrogen-Doped Graphene Sheets/MoS_2	0.1	1875/1181	1205/200/0.1 980/400/1	[6]
HC-MoS_2@GF	0.1	1397/1158	820/50/0.2	[7]
Single-layered MoS_2/carbon nanowire	0.1	1712/1267	1007/100/1 661/1000/10	[8]
CNT/MoS_2 tubular nanohybrid	0.1	1320/941	1100/100/0.5 800/1000/5	[9]
Hollow MoS_2 nanotubes	0.1	1197/896	727/100/0.1	[10]

Reference

(1) Chen, G.; Wang, S. P.; Yi, R.; Tan, L. F.; Li, H. B.; Zhou, M.; Yan, L. T.; Jiang, Y. B.; Tan, S.; Wang, D. H.; *et al*. Facile Synthesis of Hierarchical MoS_2-Carbon Microspheres as a Robust Anode for Lithium Ion Batteries. *J. Mater. Chem. A* **2016**, *4*, 9653–9660.

(2) Bai, Z. C.; Zhang, Y. H.; Zhang, Y. W.; Guo, C. L.; Tang, B. Hierarchical MoS_2@Carbon Microspheres as Advanced Anodes for Li-Ion Batteries. *Chem.-Eur. J.* **2015**, *21*, 18187–18191.

(3) Zhang, L.; Wu, H. B.; Yan, Y.; Wang, X.; Lou, X. W. Hierarchical MoS_2 Microboxes Constructed by Nanosheets with Enhanced Electrochemical Properties for Lithium Storage and Water Splitting. *Energ. Environ. Sci.* **2014**, *7*, 3302–3306.

(4) Sun, Z.; Yao, Y. C.; Wang, J.; Song, X. F.; Zhang, P.; Zhao, L. P.; Gao, L. High Rate Lithium-Ion Batteries from Hybrid Hollow Spheres with a Few-Layered MoS_2-Entrapped Carbon Sheath Synthesized by a Space-Confined Reaction. *J. Mater. Chem. A* **2016**, *4*, 10425–10434.

(5) Wan, Z. M.; Shao, J.; Yun, J. J.; Zheng, H. Y.; Gao, T.; Shen, M.; Qu, Q. T.; Zheng, H. H. Core-Shell Structure of Hierarchical Quasi-Hollow MoS_2 Microspheres Encapsulated Porous Carbon as Stable Anode for Li-Ion Batteries. *Small* **2014**, *10*, 4975–4981.

(6) Shan, T. T.; You, S. X.; Y.; Cong, H. P.; Yu, S. H.; Manthiram, A. Combining Nitrogen-Doped Graphene Sheets and MoS_2: A Unique Film-Foam-Film Structure for Enhanced Lithium Storage. *Agnew. Chem. Int. Edit.* **2016**, 128, *6*, 12975–12980.

(7) Wang, J.; Liu, J. L.; Chao, D. L.; Yan, J. X.; Lin, J. Y.; Shen, Z. X. Self-Assembly of Honeycomb-Like MoS_2 Nanoarchitectures Anchored into Graphene Foam for Enhanced Lithium-Ion Storage. *Adv. Mater.* **2014**, *26*, 7162–7169.

(8) Zhu, C.; Mu, X.; van Aken, P. A.; Yu, Y.; Maier, J. Single-Layered Ultrasmall Nanoplates of MoS_2 Embedded in Carbon Nanofibers with Excellent Electrochemical Performance for Lithium and Sodium Storage. *Angew. Chem. Int. Edit.* **2014**, *53*, 2152–2156.

(9) Chen, Y. M.; Yu, X. Y.; Li, Z.; Paik, U.; Lou, X. W. Hierarchical MoS_2 Tubular Structures Internally Wired by Carbon Nanotubes as a Highly Stable Anode Material for Lithium-Ion Batteries. *Sci. Adv.* **2016**, *2*, e1600021.

(10) Li, G. D.; Zeng, X. Y.; Zhang, T. D.; Ma, W. Y.; Li, W. P.; Wang, M. Facile Synthesis of Hierarchical Hollow MoS_2 Nanotubes as Anode Materials for High-Performance Lithium-Ion Batteries. *Crystengcomm* **2014**, *16*, 10754–10759.